crystals

MDPI

Article

Self-Healing of Cementitious Materials via Bacteria: A Theoretical Study

Pavel Demo [1], Filip Přeučil [1], Zdeněk Prošek [2], Petra Tichá [1] and Mária Domonkos [1,*]

[1] Department of Physics, Faculty of Civil Engineering, Czech Technical University in Prague, Thákurova 7, 166 29 Praha, Czech Republic; pavel.demo@fsv.cvut.cz (P.D.); FPreucil@seznam.cz (F.P.); petra.ticha@fsv.cvut.cz (P.T.)

[2] Department of Mechanics, Faculty of Civil Engineering, Czech Technical University in Prague, Thákurova 7, 166 29 Praha, Czech Republic; zdenek.prosek@fsv.cvut.cz

* Correspondence: maria.domonkos@fsv.cvut.cz

Abstract: Cracks on the surface of cementitious composites represent an entrance gate for harmful substances—particularly water—to devastate the bulk of material, which results in lower durability. Autogenous crack-sealing is a significantly limited mechanism due to a combination of the hydration process and calcite nucleation, and self-healing cementitious composites are a research area that require a great deal of scientific effort. In contrast to time-consuming experiments (e.g., only the preparation of an applicable bare concrete sample itself requires more than 28 days), appropriately selected mathematical models may assist in the deeper understanding of self-healing processes via bacteria. This paper presents theoretically oriented research dealing with the application of specific bacteria (*B. pseudofirmus*) capable of transforming available nutrients into calcite, allowing for the cracks on the surfaces of cementitious materials to be repaired. One of the principal objectives of this study is to analyze the sensitivity of the bacterial growth curves to the system parameters within the context of the logistic model in the Monod approach. Analytically calculated growth curves for various parameters (initial inoculation concentration, initial nutrition content, and metabolic activity of bacteria) are compared with experimental data. The proposed methodology may also be applied to analyze the growth of microorganisms of nonbacterial origin (e.g., molds, yeasts).

Keywords: self-healing concrete; calcite nucleation; bacterial growth; analytical model

Citation: Demo, P.; Přeučil, F.; Prošek, Z.; Tichá, P.; Domonkos, M. Self-Healing of Cementitious Materials via Bacteria: A Theoretical Study. *Crystals* **2022**, *12*, 920. https://doi.org/10.3390/cryst12070920

Academic Editors: Carmen Rizzo, Angelina Lo Giudice, Dawei Wang and Abel Moreno

Received: 30 April 2022
Accepted: 25 June 2022
Published: 29 June 2022

1. Introduction

Microorganisms (e.g., molds, bacteria, yeasts) are omnipresent in the environment and represent the prevailing form of life on Earth. In addition to their undesirable effects terminating the biodeterioration of human needs (e.g., molds vs. the food industry or building structures), microorganisms may also effectively serve as an integral part of advanced technologies. The ability of a large community of bacteria to transform a suitable nutrient source into insoluble calcite crystallites—known as microbially induced calcium carbonate precipitation (MICP)—has been used as a part of biotechnologies representing an alternative to traditionally applied methods. Among others, MICP is exploited in dentistry [1], soil bioconsolidation [2–4], grouting technologies [5,6], water remediation [7,8], conservation of stone artworks [9,10], and, in particular, civil engineering [11–15]. The formation of calcium carbonate ($CaCO_3$) requires the presence of sufficiently high concentrations of calcium cations (Ca^{2+}) and carbonate anions with a saturation level greater > 1 [16]. This biocalcification process is strongly influenced by the protonation (pH) of the system, the concentration of dissolved inorganic carbon, the concentration of calcium ions, and the number of available nucleation sites [17]. It can proceed via two basic pathways [18]: the heterotrophic mechanism, which involves sulfur or nitrogen cycles, and autotrophic calcification, which is associated with oxidation of methane and oxygen or anoxygenic

photosynthesis resulting in the formation of insoluble calcite (in the heterotrophic case, which allow for less stable polymorphs, aragonite or dolomite, to be formed [17]).

The metabolic ability of bacteria to convert organic substances to produce $CaCO_3$ as a by-product exhibits high application potential in civil engineering in the repair of cement-based materials. Cracks are one of the principal causes, allowing the penetration of aggressive liquids into the material through its surface leading to its gradual deterioration. Repairing the cracks using chemicals (e.g., latex emulsions, epoxy resins, and polyurethane-based polymers) may be applied only in the case of visible or accessible cracks; moreover, harmful gasses can be released from repaired places and repair effects are often not permanently stable. Since MICP is an environmentally friendly method (nontoxic and pollution-free), it appears to be more acceptable for the consolidation of the surface of cementitious materials [19,20].

In this field of research, there are many detailed studies dealing with related subproblems, for example, the application of self-healing techniques [21], the selection of suitable bacteria species [15,22], and the optimal location of the bacterial inoculate on the material surface [23]. It must be clarified, however, that the analytical solutions of balance equations modelling the bacterial growth followed by subsequent analysis of the influence of external/internal conditions on the growth curves is not frequently applied in the literature.

The usefulness of bacteria in the remediation process is at least twofold: they control the saturation rate of negatively charged carbonate anions, and bacterial surfaces may also serve as active sites for heterogeneous nucleation of calcium carbonate clusters [24]. Consequently, higher levels of bacteria concentration allow for a higher density of newly formed calcium carbonate clusters within the crack, resulting in an increase in the compressive strength and stiffness of the sample. Since carbonatogenesis mainly occurs intensively during the exponential phase of bacteria proliferation, it is important to control this part of the bacterial growth curve by parameters that are adjustable from the outside. The principal objective of the presented study is to theoretically follow the predictive microbiology and model the sensitivity of the exponential stage of bacterial growth on such individual parameters. However, it should be noted that in this field of research there exist many detailed studies dealing with related subproblems—for example, the application of self-healing techniques [21], the selection of suitable bacteria species [15,22], and the optimal location of the bacterial inoculate on the material surface [23]—but analytical solutions of balance equations modelling bacterial growth followed by subsequent analysis of the influence of external/internal conditions on the growth curves are not frequently applied in the literature. It remains to be studied whether or not the bacterial growth curve can serve as an acceptable predictive indicator that allows one to estimate the rate of carbonate formation in cracked concrete.

2. Experimental Section

To illustrate the self-healing ability of calcifying microorganisms, we tested *Bacillus pseudofirmus* to repair the cracks on the surface of a 2-year-old cement paste (stored under laboratory conditions under 50% humidity and at 30 °C). Cracks were simulated by grooves prepared with a scalpel. The resulting artificial crack was 0.25 mm wide. The capability of bacterial crack self-healing was closely connected (besides the chosen bacterial genus) with the concentration of newly formed bacteria and environmental conditions (e.g., temperature, number density of present free calcium cations, pH factor, etc.) and an analysis of these parameters is out of the scope of this paper. Before the application of the bacteria culture, the surface of the sample was polished with both SiC media of different roughnesses and with diamond paste to allow for better observation of the resulting calcified structures. Finally, 0.05 mL of a bacteria-containing medium was implanted into the examined cracks and then the sample was placed in a desiccator (99% humidity) to prevent the medium from dehydration.

Calcified structures on the surfaces of samples were monitored using (i) the ZEISS Axio Zoom V16 Stereo Zoom Microscope for Large Fields for optical microscopy and

(ii) the FEG Merlin ZEISS scanning electron microscope (SEM) for microscopic structural and elemental analysis. Figure 1 represents the gradual filling process of the artificial crack with the newly formed calcite structure. As can be seen, bacteria form crystal clusters in sizes ranging from 50 to 100 microns, and the crystal clusters have paraboloid-like shapes. The higher magnification of the same area (Figure 2) shows that the cluster itself consists of microcrystals ranging from 1 to 2 microns in size. In contrast, it can be seen in the sample without bacteria (Figure 2) that there are no clusters; rather, larger crystals up to 20 µm in size are formed.

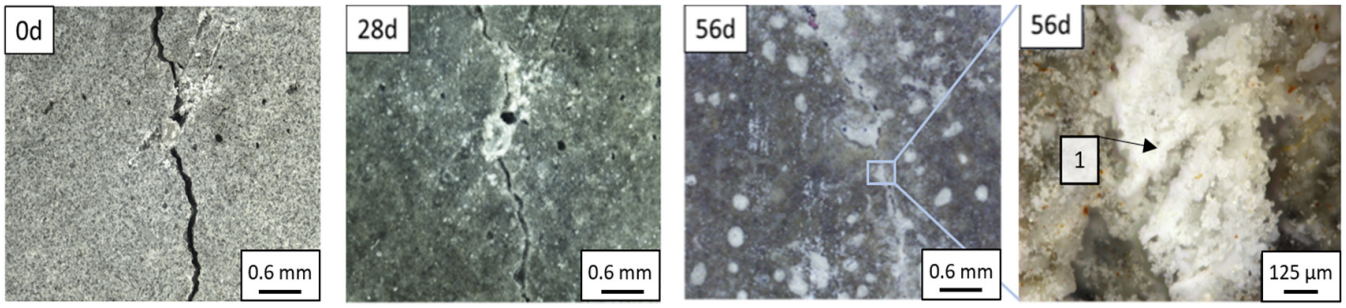

Figure 1. Optical images of the crack healing process over 56 days: 1—Crystals clusters (last image magnified to 80×).

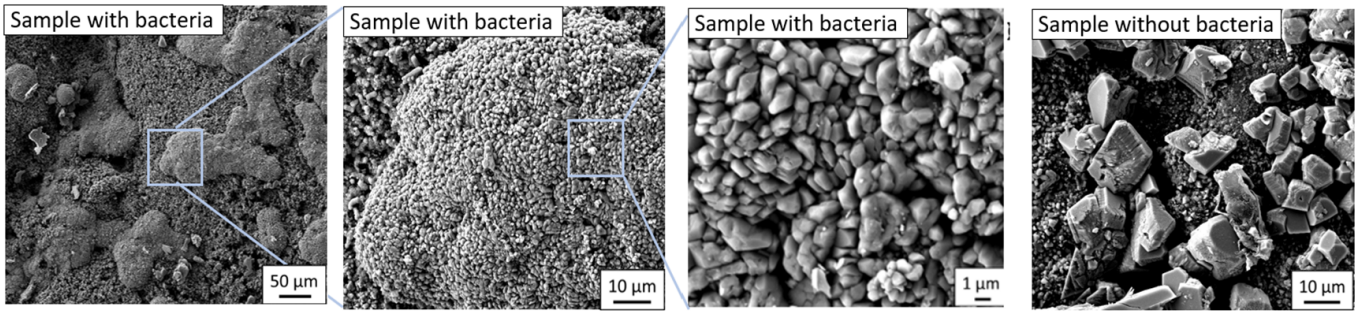

Figure 2. SEM images of the formation of new structures on the surface of cement paste (secondary electron detector).

Furthermore, according to phase analysis (using Energy Spectrometer EDS by Oxford Instruments), the newly formed structures in the cracks contained 39.8 ± 3.8 wt. % of calcium, 12.2 ± 1.0 wt. % of carbon and 45.9 ± 5.3 wt. % of oxygen, corresponding to the crystal structure of calcite ($CaCO_3$).

It must be clarified that our research is not focused on the improvement of mechanical properties of concrete constructions; rather, it is directed to the extension of their durability.

3. Model

This theoretical study addresses an important problem that rarely emerges in research activities in this field: optimization of parameters (adjustable from the outside) resulting in maximization of bacterial growth on the surface of the building material. The principal aim is to analyze the analytical solution of the logistic growth equation using the Monod equation with subsequent maximization of the exponential part of the growth curve, where the bacterial number density exponentially increases followed by the accumulation of their metabolic products. The exponential growth phase terminates in a steady state when the balance between growth and death rates in the bacterial population is established.

In order to consolidate the surface, or bulk, of building material, the desired number of proliferating bacteria must be present in the damaged location. The cornerstone of microorganism (e.g., molds, bacteria, yeasts) growth modeling is the principle that bacteria grow when their birth rate exceeds their death rate [25,26]). It must be clarified that without

any additional conditions (such as real nutrition resource limitations or competition among individuals within species), this Malthusian model—mathematically represented by linear ordinary differential equation—leads to an uncontrollable and thus unrealistic exponential growth law for population size. For this reason, more accurate theories have been taken into account, resulting in the class of logistic-like equations (mainly in multiparametric forms; for details, see [27]) modeling the bacterial sigmoidal (S-shaped) growth curves under more appropriate regulation rules. One of the most applied models is the growth equation, which involves the functional relationship between the specific growth rate and the concentration of the limiting nutritional substrate. Monod [28] introduced this purely empirical function $f(t)$ (mathematically equivalent to the Michaelis–Menten formula describing enzyme kinetics in biochemistry) in order to better coincide with the experimental data:

$$f(t) = \frac{r_m \cdot S}{(a + S)} \tag{1}$$

where $S = S(t)$ is the concentration of nutrients, r_m stands for the maximum growth rate (corresponding to the maximum difference between birth and death rates) and a is known as the Monod constant, formally corresponding to half of the maximum growth rate ($r_m/2$) when $S = a$ [29], but may be related to the interaction between the substrate and the bacteria. This characteristic represents an "energetical factor" of growth and is influenced by the interplay of diffusion rates through the bacteria membrane, the oxygen gradient within the system, the enzymatic processes, the temperature, etc. [30]. Several approaches have been focused on interpreting the Monod function by theoretically applying thermodynamic, kinetic, or statistical models [31–35]. Using the Monod function (1), one obtains a logistic-like equation in the Monod approach describing the growth of bacteria under more realistic conditions:

$$\frac{dN}{dt} = \frac{N \cdot r_m \cdot S}{(a + S)} = N \cdot f(t), \tag{2}$$

where $N(t)$ is the concentration of bacteria.

Furthermore, following the Monod assumption that the bacterial growth rate is proportional to nutrient rate consumption with opposite sign,

$$\frac{dN}{dt} = -\gamma \frac{dS}{dt} \tag{3}$$

where the proportionality coefficient γ is called the growth yield; the independent parameter reflecting the specific properties of bacteria, representing the efficiency of bacteria metabolism to process the source of nutrition (γ = bacteria formed/nutrient consumed in a unit of time) and, with the help of the Equation (2), the balance equation for nutrient rate consumption reads:

$$\gamma \frac{dS}{dt} = -N \cdot \frac{r_m \cdot S}{(a + S)} \tag{4}$$

Having determined the bacteria concentration $N(t)$, temporal dependency of the nutrient concentration may be calculated from the differential Equation (4), and vice versa.

Both balance Equations (2) and (3) have to be complemented by initial conditions (assumed to be known from experiments expressed by evidently independent values of initial concentrations of bacteria inoculation, and of nutrient source):

$$N(t = 0) = N_o, \;\; S(t = 0) = S_o \tag{5}$$

Integrating the sum of Equations (2) and (4) with using the initial conditions (5) we obtain:

$$N(t) + \gamma \cdot S(t) = N_o + \gamma \cdot S_o = k \tag{6}$$

Finally, taking into account Equations (2) and (6), the solution of ordinary differential equation for bacteria concentration $N(t)$ can be expressed as follows:

$$t(N) = \frac{(k + a \cdot \gamma)}{r_m \cdot k} \cdot \ln\left(\frac{N}{N_o}\right) - \frac{a \cdot \gamma}{r_m \cdot k} \cdot \ln\left(\frac{N - k}{N_o - k}\right) \quad (7)$$

with asymptotes $N = 0$, $N = k$, where k is defined by the relationship (6). It can be readily understood that the above solution involves five independent input parameters: N_o, S_o, γ, a, r_m. Similar growth curves can be obtained from solution of the Luedeking–Piret equation [36] or from analysis of batch fermentation problems [37].

4. Results and Discussion

Solution (7) of the logistic equation (in the Monod formulation) was used in order to determine the sensitivity of the growth curves to various input parameters (N_o, S_o, γ, a, r_m) for *Bacillus pseudofirmus*, grown under laboratory conditions with an initial inoculation concentration of 0.033 g/L and at a temperature of 30 °C. All modeled growth curves below correspond to the set of baseline parameters (N_o = 0.033 g/L, S_o = 0.8 g/L, γ = 0.2, r_m = 4 h^{-1}, a = 60 g/L) used in our previous, numerically oriented publication [38]. Typical growth curves for various initial concentrations of inoculate N_o, resp. nutrient source S_o are shown in Figures 3 and 4.

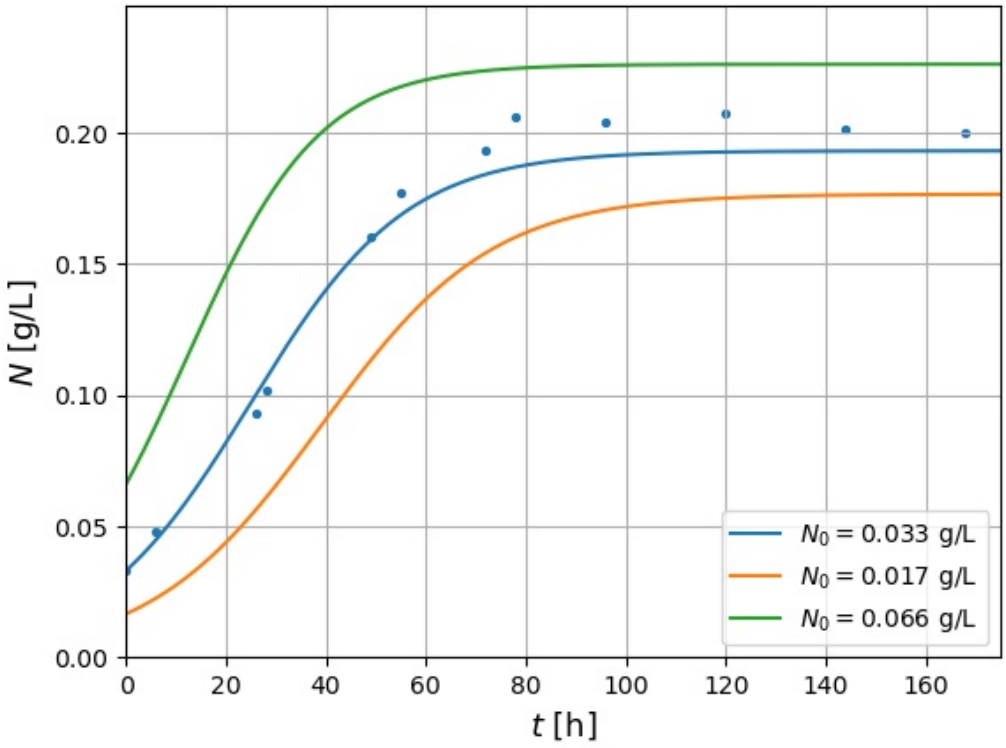

Figure 3. Dependence of bacteria concentration $N(t)$ on various concentrations of the inoculate. All independent parameters (a = 60 g/L, r_m = 4 h^{-1}, γ = 0.2, and S_o = 0.8 g/L) were kept constant. Blue dots correspond to the experimental data.

As expected, the parameters controllable from the outside (N_o, S_o) directly govern both the bacterial growth rate and the maximally reachable concentration of bacteria within the system: the larger the inoculation/initial nutrient concentrations, the higher the values of maximal bacteria amount can be produced with higher growth rates (see the slopes of the appropriate growth curves in Figures 3 and 4).

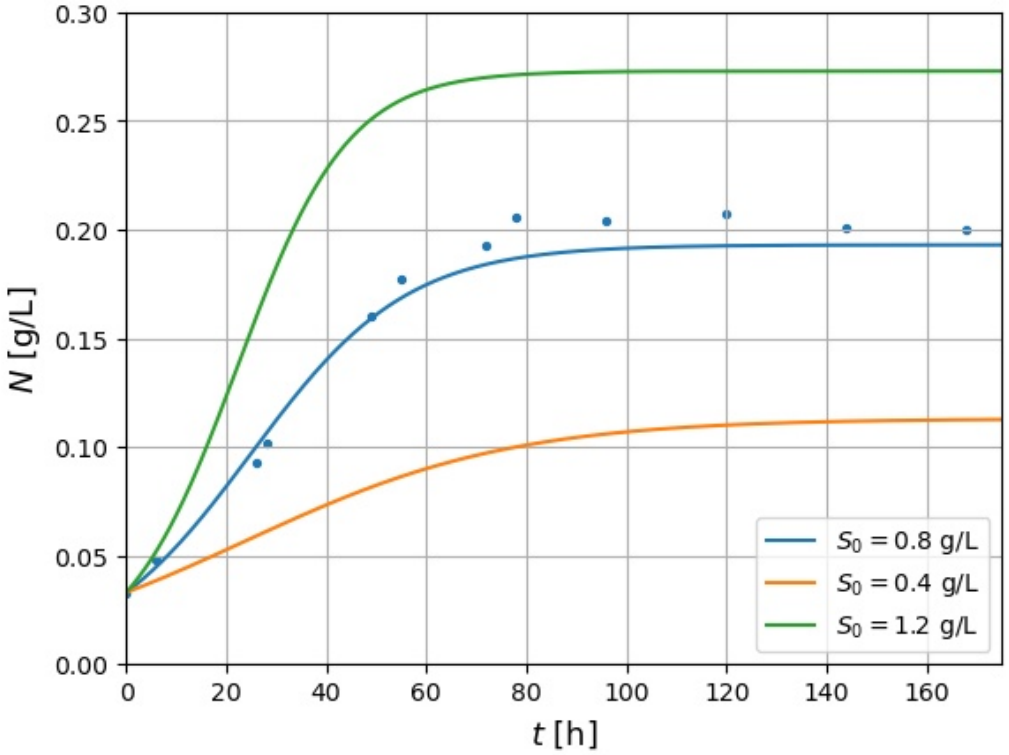

Figure 4. Dependence of bacteria concentration $N(t)$ on different initial concentrations of nutrient source. All the independent parameters (a = 60 g/L, r_m = 4 h^{-1} and γ = 0.2, and N_o = 0.033 g/L). Blue dots correspond to the experimental data.

However, our systematic interest is focused on a more detailed analysis of the influence of input parameters γ, r_m, a (connected with the inner metabolic activity of the chosen bacteria species) on both the time evolution of bacteria and nutrient concentrations (see Figures 5–7).

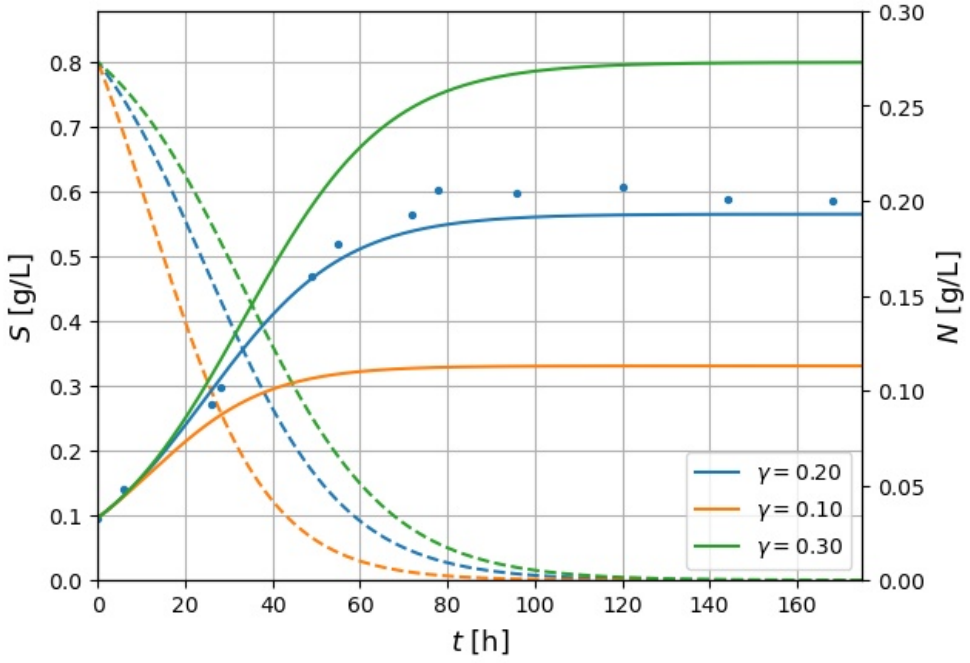

Figure 5. Sensitivity of bacterial concentration on the inner parameter γ (a = 60 g/L and r_m = 4 h^{-1}). Blue dots correspond to experimental data.

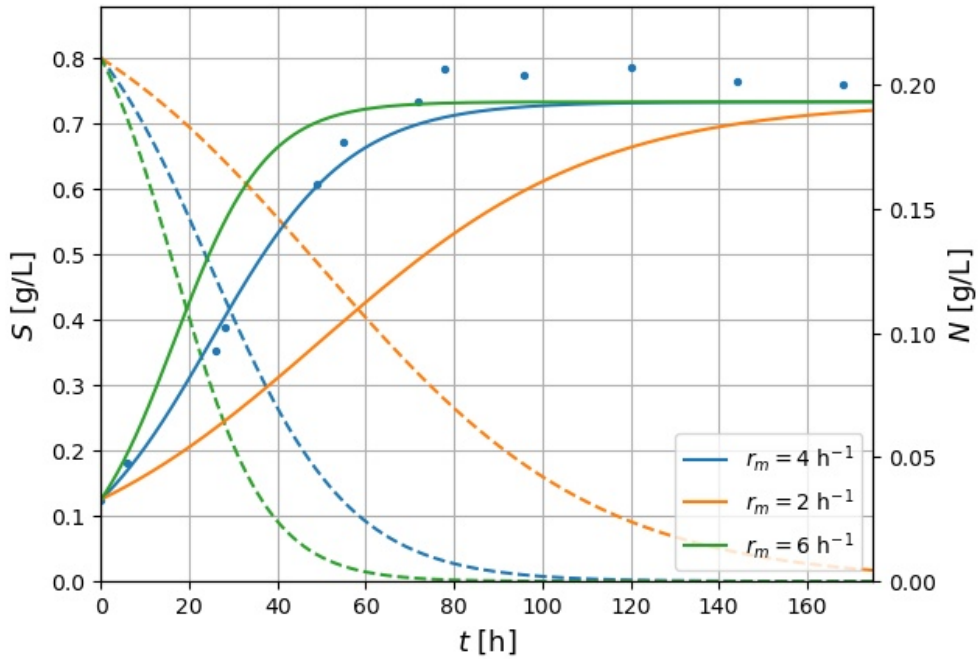

Figure 6. Influence of the maximal growth rate r_m on the growth curves ($\gamma = 0.2$ and $a = 60$ g/L). Blue dots represent experimental data.

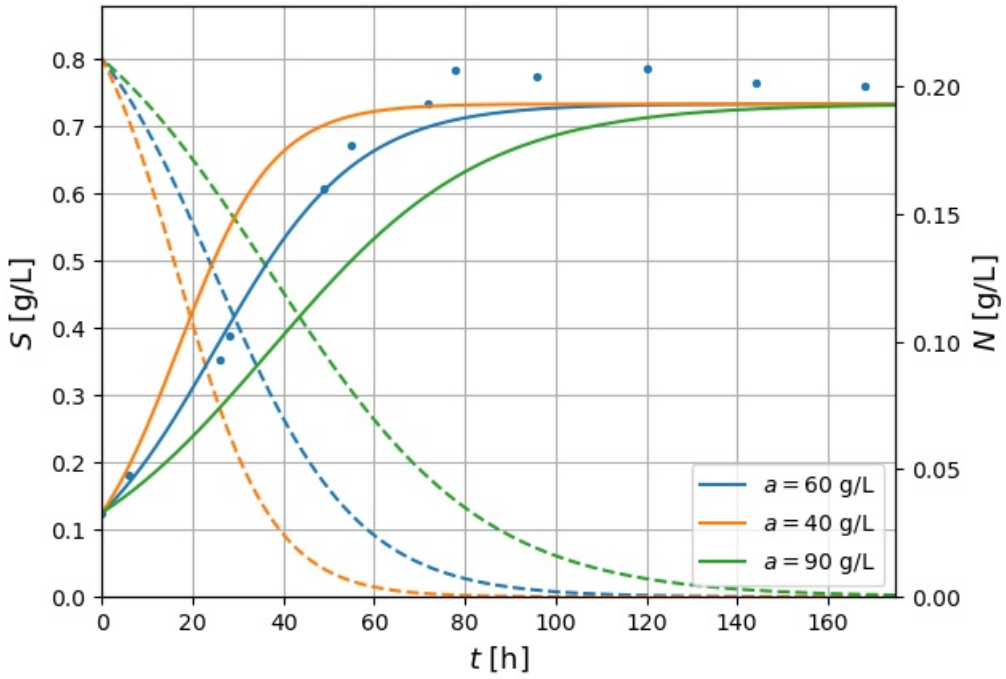

Figure 7. Dependence of $N(t)$ on half saturation characteristics a ($\gamma = 0.2$ and $r_m = 4\ h^{-1}$). Blue dots are experimental data.

Using expression (7), one may obtain a set of growth curves representing the influence of the inner parameters γ, r_m, a (with given experimental input: $N_o = 0.033$ g/L and $S_o = 0.8$ g/L) on their time evolution.

One of the essential characteristics of the metabolic ability of bacteria is the parameter γ, demonstrating their efficiency in nutrient source processing; in Monod formulation, "the growth yield" [28]: γ units of bacteria cells are formed from one unit of the consumed nutrition source modifying the composition of the substrate. This process consists of two steps: transport of the required nutrition to the bacterial cell, followed by metabolic

processes that result in a newly formed bacterial cell as a consequence of the substrate consumption. As can be seen in Figure 5, this parameter also has an indispensable impact on the maximum bacterial concentration. It must be clarified, however, that for sufficiently high values of γ the bacterial growth can be satisfactorily modeled within the context of the appropriate "pure" logistic equations [37].

The half saturation concentration of nutrients, a (Monod constant), exhibits a weak influence on the resulting maximal concentration of newly formed bacteria—similarly, as the rate limit for increasing bacteria concentration r_m—(see Figure 7) but has an indispensable impact on the exponential growth phase (Figure 8).

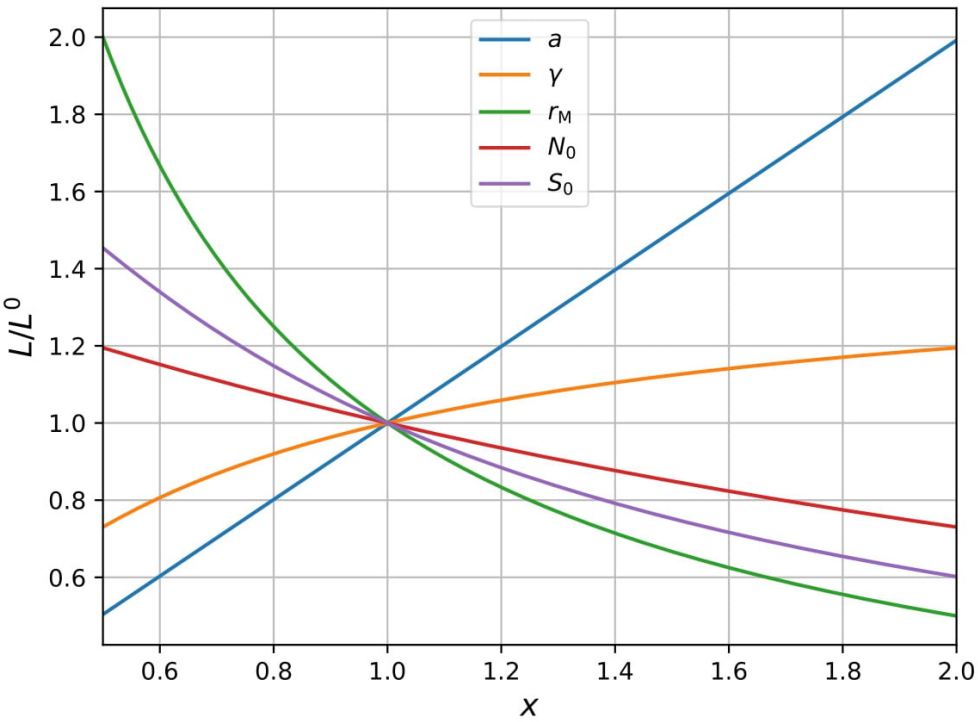

Figure 8. Influence of external (N_o, S_o) and internal (γ, r_m, a) free parameters on the length L of the linearized part of the exponential phase of the growth curve (see Formula (11)). Here, L is scaled by L_o ($x = L/L_o$) where L_o corresponds to the set (a = 60 g/L, γ = 0.2, r_m = 4 h^{-1}, N_o = 0.033 g/L, S_o = 0.8 g/L).

The analysis of the inner parameters influence on the behavior of the exponential part of the sigmoidal growth curve, where the division of bacteria is most intensive, is compelling. The bacteria massively proliferates in this region, rapidly increasing their concentration and resulting in an amplification of the self-healing process; thus, the length of the exponential part of the growth curve straightforwardly influences the amount of number density of bacteria: the longer exponential part leads to the higher concentration of bacteria, and vice versa. To quantify this length, let us expand the growth curve in the Taylor series around the inflection point N_i,

$$N_i = (k + a{\cdot}\gamma) - \sqrt{a{\cdot}\gamma{\cdot}(k + a{\cdot}\gamma)} \tag{8}$$

and consider only a linear part of this expansion. The length L of this linearized part (connecting the points N_o and k, respectively) can be easily determined to be

$$L^2 = (k - N_O)^2{\cdot}\left[1 + \frac{1}{r_m^2{\cdot}(2N_i - k)^2}\right] \tag{9}$$

where the slope of the exponential part of growth curve taken at inflection point is

$$\frac{dN_i}{dt} = r_m \cdot (2N_i - k). \tag{10}$$

Finally, the length L can be expressed with the help of Formula (10) as

$$L = \gamma \cdot S_o \cdot \sqrt{1 + \frac{1}{r_m^2 \cdot \left[(k + 2a \cdot \gamma) - 2\sqrt{a \cdot \gamma (k + a \cdot \gamma)}\right]^2}} \tag{11}$$

The sensitivity of the bacterial growth curves on changes of the input parameters is shown in Figure 8, where x is a given ratio of changed and unchanged parameters, where $x \in (0.5, 2)$ has been applied; thus, $x = 1$ corresponds to the lengths $L = L_o$ of the linearized exponential growth phase for a set of baseline parameters. As an alternative example, $L(x \cdot N_o, S_o, \gamma, a, r_m)$ reflects the sensitivity of the linearized part of the exponential growth phase to the change of inoculate concentration. The figure above especially confirms the relevance of bacterial metabolic ability on the prolongation of the exponential part of growth.

For technologies applying bacteria as the self-healing agents, there emerge two principal questions in order to optimize their standardization methodologies: (1) what parameters basically influence the attainable concentration maximum of newly formed microorganisms, max $N(t)$, in the system, and (2) what parameters have an impact to the extension of the exponential stage of bacteria proliferation in the system? Within the context of our model, five free (independent) parameters play a key role in the bacteria growth process. Although the initial concentrations of inoculum N_o and nutrient source S_o may be adjusted arbitrarily from the outside at the beginning of the experiment, the remaining parameters (γ, r_m, a) characterize the intrinsic properties of a particular bacterium closely connected with its metabolism, membrane transport, and other microbiological activities. Sensitivity to changes in individual parameters for the growth curve follows from analysis of the solution (7). The maximum concentration max $N(t)$ is practically insensitive to the change of two internal parameters: the maximum growth rate, r_m, and the Monod constant, a. In both cases, when r_m varied from 2 to 6 per hour and a from 40 g/L to 90 g/L, the value of max $N(t)$ reads 0.19 g/L (as demonstrated in Figures 6 and 7). Conversely, the above parameters strongly affect the length of exponential phase of bacteria proliferation (Figure 8). In the case of maximum growth rate changes, the bacteria concentration $N(t)$ converges to max $N(t)$ from 80 h to more than 180 h (Figure 6), while changes in the Monod constant result in the extension of an exponential part of the growth curve from 70 to 150 h (Figure 7).

As expected qualitatively, the higher the initial concentrations of inoculum resp. nutrient source, the higher max $N(t)$. Quantitatively, both external parameters have a direct impact on the maximum bacteria concentration. Changes in initial nutrient concentrations from 0.4 g/L to 1.2 g/L result in an increase in max $N(t)$ from 0.11 g/L to 0.27 g/L. (as represented in Figure 4) while the changes of the initial concentrations of inoculate correspond to changes in maximum concentration max $N(t)$ from 0.17 g/L to 0.24 g/L (Figure 3).

Finally, the growth curve of the bacterial colonies is also sensitive to the growth yield γ reflecting the efficiency of the bacterial metabolism of nutrient processing. As follows from Figures 5 and 8, the higher γ, the higher the values of max $N(t)$: an increase in metabolism of nutrient processing from 0.1 to 0.3 leads to increase in max $N(t)$ from 0.125 g/L to 0.275 g/L.

The answer to the second question mentioned above can be found in illustrative Figure 8: when the input parameters increase compared to the baseline set of parameters (i.e., for $x > 1$), then only the increased Monod constant a and growth yield γ result in extension of the exponential phase of bacteria proliferation; the remaining parameters lowered the exponential part of the growth curve. Conversely, when the input parameters are lowered, the opposite effect occurs. For example, for the initial concentrations of the inoculum < 0.033 g/L (=baseline value) the length of the exponential part of the growth

curve is more extended (see also Figure 4). Similarly, for initial concentrations of the nutrient source < 0.8 g/L the exponential phase of bacterial proliferation converges to max $N(t)$ very slowly.

It is found that within the context of the logistic equation in the Monod approach (comprising all parameters with the straightforward microbiological meaning), it is possible to model the growth curves of *B. pseudofirmus* (as a self-healing agent in concrete) depending on basic external/intrinsic parameters and to estimate their technological relevance.

5. Conclusions

Microbially induced calcium carbonate precipitation (MICP) has been applied over a decade as a self-healing technique for the consolidation of damaged localities on surfaces (resp. in bulks) of building materials. The ability of certain bacteria species (here, *B. pseudofirmus*) to transform nutrient sources into insoluble crystallites of calcite is exploited to fill the cracks to form a protective layer on the damaged surface of the concrete. Consequently, controllable division (growth) of microorganisms is crucial for an optimal self-healing process.

In addition to modeling of bacteria growth based on the first principles approach, one of the useful sources of required knowledge is the application of logistic-like equations in the Monod formulation [39]. The analytical solution presented in this paper allows one to determine the influence of both external parameters (represented by adjustable initial concentrations of the inoculate and nutrient source, respectively) and internal bacteria properties (related to their metabolic activities) on the growth curves of bacteria. In particular, the efficiency of the bacteria metabolism ability to process the source of nutrition can markedly affect the value of maximal bacteria concentration.

It must be clarified, however, that the validity of our methodology is not limited to bacterial growth curves, but can also be applied on other types of microorganisms (especially for growth of molds).

Author Contributions: Conceptualization, P.D.; methodology, P.D. and F.P.; formal analysis, F.P.; investigation, Z.P.; writing—original draft preparation, P.D. and M.D.; writing—review and editing, P.T.; visualization, M.D. and P.T. All authors have read and agreed to the published version of the manuscript.

Funding: This research was funded by the Czech Science Foundation, grant no. GA22-06621S.

Institutional Review Board Statement: Not applicable.

Informed Consent Statement: Not applicable.

Data Availability Statement: The data presented in this study are available on request from the corresponding author.

Acknowledgments: The authors wish to thank Pavla Ryparova at the Czech Technical University in Prague for providing the experimental growth curve of *B. pseudofirmus*.

Conflicts of Interest: The authors declare no conflict of interest.

References

1. Seifan, M.; Sarabadani, Z.; Berenjian, A. Microbially Induced Calcium Carbonate Precipitation to Design a New Type of Bio Self-Healing Dental Composite. *Appl. Microbiol. Biotechnol.* **2020**, *104*, 2029–2037. [CrossRef] [PubMed]
2. Tang, C.-S.; Yin, L.; Jiang, N.; Zhu, C.; Zeng, H.; Li, H.; Shi, B. Factors Affecting the Performance of Microbial-Induced Carbonate Precipitation (MICP) Treated Soil: A Review. *Environ. Earth Sci.* **2020**, *79*, 94. [CrossRef]
3. Jiang, N.; Tang, C.; Hata, T.; Courcelles, B.; Dawoud, O.; Singh, D.N. Bio-mediated Soil Improvement: The Way Forward. *Soil Use Manag.* **2020**, *36*, 185–188. [CrossRef]
4. Almajed, A.; Lateef, M.A.; Moghal, A.A.B.; Lemboye, K. State-of-the-Art Review of the Applicability and Challenges of Microbial-Induced Calcite Precipitation (MICP) and Enzyme-Induced Calcite Precipitation (EICP) Techniques for Geotechnical and Geoenvironmental Applications. *Crystals* **2021**, *11*, 370. [CrossRef]
5. Liu, J.; Li, G.; Li, X. Geotechnical Engineering Properties of Soils Solidified by Microbially Induced CaCO3 Precipitation (MICP). *Adv. Civ. Eng.* **2021**, *2021*, 6683930. [CrossRef]

6. Deng, X.; Li, Y.; Liu, H.; Zhao, Y.; Yang, Y.; Xu, X.; Cheng, X.; Wit, B. de Examining Energy Consumption and Carbon Emissions of Microbial Induced Carbonate Precipitation Using the Life Cycle Assessment Method. *Sustainability* **2021**, *13*, 4856. [CrossRef]
7. Hu, L.; Wang, H.; Xu, P.; Zhang, Y. Biomineralization of Hypersaline Produced Water Using Microbially Induced Calcite Precipitation. *Water Res.* **2021**, *190*, 116753. [CrossRef]
8. Wang, Z.; Su, J.; Ali, A.; Zhang, R.; Yang, W.; Xu, L.; Zhao, T. Microbially Induced Calcium Precipitation Based Simultaneous Removal of Fluoride, Nitrate, and Calcium by Pseudomonas Sp. WZ39: Mechanisms and Nucleation Pathways. *J. Hazard. Mater.* **2021**, *416*, 125914. [CrossRef]
9. Marvasi, M.; Mastromei, G.; Perito, B. Bacterial Calcium Carbonate Mineralization in Situ Strategies for Conservation of Stone Artworks: From Cell Components to Microbial Community. *Front. Microbiol.* **2020**, *11*, 1386. [CrossRef]
10. Ortega-Morales, B.O.; Gaylarde, C.C. Bioconservation of Historic Stone Buildings—An Updated Review. *Appl. Sci.* **2021**, *11*, 5695. [CrossRef]
11. Yatish Reddy, P.V.; Ramesh, B.; Prem Kumar, L. Influence of Bacteria in Self Healing of Concrete—A Review. *Mater. Today Proc.* **2020**, *33*, 4212–4218. [CrossRef]
12. Su, Y.; Zheng, T.; Qian, C. Application Potential of Bacillus Megaterium Encapsulated by Low Alkaline Sulphoaluminate Cement in Self-Healing Concrete. *Constr. Build. Mater.* **2021**, *273*, 121740. [CrossRef]
13. Rong, H.; Wei, G.; Ma, G.; Zhang, Y.; Zheng, X.; Zhang, L.; Xu, R. Influence of Bacterial Concentration on Crack Self-Healing of Cement-Based Materials. *Constr. Build. Mater.* **2020**, *244*, 118372. [CrossRef]
14. Justo-Reinoso, I.; Heath, A.; Gebhard, S.; Paine, K. Aerobic Non-Ureolytic Bacteria-Based Self-Healing Cementitious Composites: A Comprehensive Review. *J. Build. Eng.* **2021**, *42*, 102834. [CrossRef]
15. Sri Durga, C.S.; Ruben, N.; Sri Rama Chand, M.; Indira, M.; Venkatesh, C. Comprehensive Microbiological Studies on Screening Bacteria for Self-Healing Concrete. *Materialia* **2021**, *15*, 101051. [CrossRef]
16. Mondal, S.; Ghosh, A. Review on Microbial Induced Calcite Precipitation Mechanisms Leading to Bacterial Selection for Microbial Concrete. *Constr. Build. Mater.* **2019**, *225*, 67–75. [CrossRef]
17. Hammes, F.; Verstraete, W. Key Roles of PH and Calcium Metabolism in Microbial Carbonate Precipitation. *Rev. Environ. Sci. Biotechnol.* **2002**, *1*, 3–7. [CrossRef]
18. Castanier, S.; Le Métayer-Levrel, G.; Perthuisot, J.-P. Ca-Carbonates Precipitation and Limestone Genesis—The Microbiogeologist Point of View. *Sediment. Geol.* **1999**, *126*, 9–23. [CrossRef]
19. Al-Salloum, Y.; Hadi, S.; Abbas, H.; Almusallam, T.; Moslem, M.A. Bio-Induction and Bioremediation of Cementitious Composites Using Microbial Mineral Precipitation—A Review. *Constr. Build. Mater.* **2017**, *154*, 857–876. [CrossRef]
20. Luo, M.; Jing, K.; Bai, J.; Ding, Z.; Yang, D.; Huang, H.; Gong, Y. Effects of Curing Conditions and Supplementary Cementitious Materials on Autogenous Self-Healing of Early Age Cracks in Cement Mortar. *Crystals* **2021**, *11*, 752. [CrossRef]
21. Kumar Jogi, P.; Vara Lakshmi, T.V.S. Self Healing Concrete Based on Different Bacteria: A Review. *Mater. Today Proc.* **2021**, *43*, 1246–1252. [CrossRef]
22. Brasileiro, P.P.F.; Brandao, Y.B.; Sarubbo, L.A.; Benachour, M. Self-Healing Concrete: Background, Development, and Market Prospects. *Biointerface Res. Appl. Chem.* **2021**, *11*, 14709–14725. [CrossRef]
23. Qian, C.; Zheng, T.; Zhang, X.; Su, Y. Application of Microbial Self-Healing Concrete: Case Study. *Constr. Build. Mater.* **2021**, *290*, 123226. [CrossRef]
24. Ghosh, T.; Bhaduri, S.; Montemagno, C.; Kumar, A. Sporosarcina Pasteurii Can Form Nanoscale Calcium Carbonate Crystals on Cell Surface. *PLoS ONE* **2019**, *14*, e0210339. [CrossRef]
25. Advanced Engineering Mathematics, 6th Edition [Book]. Available online: https://www.oreilly.com/library/view/advanced-engineering-mathematics/9781284105971/ (accessed on 25 April 2022).
26. Winkel, B. 2017-Stan, Guy-Bart—Modelling in Biology. Class Notes. Imperial College of London. 2017. Available online: https://www.simiode.org/resources/3701/download/2017Stan_ModellingInBiology.pdf (accessed on 28 June 2022).
27. Panik, M.J. *Growth Curve Modeling: Theory and Applications*; Wiley: Hoboken, NJ, USA, 2014; ISBN 978-1-118-76404-6.
28. Monod, J. The Growth of Bacterial Cultures. *Annu. Rev. Microbiol.* **1949**, *3*, 371–394. [CrossRef]
29. Liu, Y.; Lin, Y.-M.; Yang, S.-F. A Thermodynamic Interpretation of the Monod Equation. *Curr. Microbiol.* **2003**, *46*, 233–234. [CrossRef]
30. Vivekanandan, B.; Rao, A.S. Estimation of Yield, Growth Rate, Decay Rate, and Half-Saturation Coefficients of ASM1 Model Parameters. *Int. J. Environ. Res.* **2017**, *11*, 415–423. [CrossRef]
31. Ugalde-Salas, P.; Desmond-Le Quéméner, E.; Harmand, J.; Rapaport, A.; Bouchez, T. Insights from Microbial Transition State Theory on Monod's Affinity Constant. *Sci. Rep.* **2020**, *10*, 5323. [CrossRef]
32. Desmond-Le Quéméner, E.; Bouchez, T. A Thermodynamic Theory of Microbial Growth. *ISME J.* **2014**, *8*, 1747–1751. [CrossRef]
33. Saadat, N.; Nies, T.; Rousset, Y.; Ebenhöh, O. Thermodynamic Limits and Optimality of Microbial Growth. *Entropy* **2020**, *22*, 277. [CrossRef]
34. Alvarez-Ramirez, J.; Meraz, M.; Jaime Vernon-Carter, E. A Theoretical Derivation of the Monod Equation with a Kinetics Sense. *Biochem. Eng. J.* **2019**, *150*, 107305. [CrossRef]
35. Liu, Y. Overview of Some Theoretical Approaches for Derivation of the Monod Equation. *Appl. Microbiol. Biotechnol.* **2007**, *73*, 1241–1250. [CrossRef] [PubMed]

36. Garnier, A.; Gaillet, B. Analytical Solution of Luedeking-Piret Equation for a Batch Fermentation Obeying Monod Growth Kinetics: Solution of Monod-Luedeking-Piret Equations. *Biotechnol. Bioeng.* **2015**, *112*, 2468–2474. [CrossRef] [PubMed]
37. Xu, P. Analytical Solution for a Hybrid Logistic-Monod Cell Growth Model in Batch and Continuous Stirred Tank Reactor Culture. *Biotechnol. Bioeng.* **2020**, *117*, 873–878. [CrossRef] [PubMed]
38. Nežerka, V.; Demo, P.; Schreiberová, H.; Ryparová, P.; Bílý, P. Self-Healing Concrete: Application of Monod's Approach for Modeling *Bacillus pseudofirmus* Growth Curves. *Eur. J. Environ. Civ. Eng.* **2022**, 1–13. [CrossRef]
39. Fernandez, C.A.; Correa, M.; Nguyen, M.-T.; Rod, K.A.; Dai, G.L.; Cosimbescu, L.; Rousseau, R.; Glezakou, V.-A. Progress and Challenges in Self-Healing Cementitious Materials. *J. Mater. Sci.* **2021**, *56*, 201–230. [CrossRef]